P1.31 DETERMINATION OF 3-D CLOUD ICE WATER CONTENTS BY COMBINING MULTIPLE DATA SOURCES FROM SATELLITE, GROUND RADAR AND NUMERICAL MODEL

Eun-Kyoung Seo* and Guosheng Liu

Florida State University, Tallahassee, Florida

1. INTRODUCTION

One of the ARM program important goals is to develop and test radiation and cloud parameterizations of climate models using single column modeling (SCMs) (Randall et al. 1996). As forcing terms, SCMs need advection tendency of cloud condensates besides the tendencies of temperature, moisture and momentum. To compute the tendency terms of clound condensates, 3 dimensional distribution of cloud condensates over a scale much larger than the climate model's grid scale is needed. Since they can cover a large area within a short time period, satellite measurements are useful utilities to provide advection tendency of cloud condensates for SCMs. However, so far, most satellite retrieval algorithms only retrieve vertically integrated quantities, for example, in the case of cloud ice, ice water path (IWP). To fulfill the requirement of 3-D ice water content field for computing ice water advection, in this study, we develop an ice water content profile retrieval algorithm by combining the vertical distribution characteristics obtained from long-term surface radar observations and satellite high-frequency microwave observations that cover a large area. The algorithm is based on the Bayesian theorem using a priori database derived from analyzing cloud radar observations at the SGP site. The end product of the algorithm is a 3-D ice water content covering 10 deg. x 10 deg. surrounding the SGP site during the passage of the satellite. This 3-D ice water content, together with wind field analysis, can be used to compute the advection tendency of ice water for SCMs.

2. DATA

In this study, brightness temperatures (T_Bs) from from satellite Advanced Microwave Sounding Unit-B (AMSU-B) and radar reflectivities from millimeter-wave cloud radar (MMCR) and next generation radar (NEXRAD) are used during the March 2000 ARM Intensive Observation Period (IOP) over a 10° x 10° box centered at the SGP site. More details can be found in Seo and Liu (2005) for the AMSU-B and MMCR observations and modeled database having T_B-ice water content (IWC) profile relationships. For the NEXRAD radar reflectivity, level II data operating at a wavelength of 10 cm from the KINX NEXRAD located in Tulsa, Oklahoma have been used.

3. RETRIEVAL ALGORITHM

Based on Baye's theorem, the expected vector $\hat{E}(\mathbf{x})$ of $\mathbf{x}$ (in this study, IWC profile) given a set of $\mathbf{y}_0$ (in this study, the observed brightness temperatures), is approximated in a discrete form (Olson et al. 1996) as

$$\hat{E}(\mathbf{x}) = \sum_{\mathrm{j}} \mathbf{x}_{\mathrm{j}} \exp\left\{-0.5\left[\mathbf{y}_0 - \mathbf{y}_s(\mathbf{x}_{\mathrm{j}})\right]^{\mathrm{T}} (\mathbf{O}+\mathbf{S})^{-1}\left[\mathbf{y}_0 - \mathbf{y}_s(\mathbf{x}_{\mathrm{j}})\right]\right\} / \hat{A},$$

where $\mathbf{O}$ and $\mathbf{S}$ are the observation and simulation error covariance matrices, respectively, and $\hat{A}$ is the normalization factor defined as

$$\hat{A} = \sum_{\mathrm{j}} \exp\left\{-0.5\left[\mathbf{y_0} - \mathbf{y_s}(\mathbf{x}_{\mathrm{j}})\right]^{\mathrm{T}} (\mathbf{O}+\mathbf{S})^{-1}\left[\mathbf{y_0} - \mathbf{y_s}(\mathbf{x}_{\mathrm{j}})\right]\right\}$$

Here $\mathbf{x}_{\mathrm{j}}$ represent the *j*th IWC profile in the modeled database and $\mathbf{y}_s(\mathbf{x}_j)$ is a brightness temperature vector simulated by a radiative transfer model (Liu 2004) for $\mathbf{x}_{\mathrm{j}}$. Using $\hat{E}(\mathbf{x})$, IWC profiles have been retrieved from the AMSU-B T_Bs.

4. HORIZONTAL STRUCTURE OF AMSU-B AND NEXRAD IWPS

A horizontal picture of IWP distribution has been obtained from the AMSU-B and the NEXRAD retrievals (Fig. 1). For the NEXRAD retrievals, IWCs at each layer are derived from vertical NEXRAD radar reflectivity using $IWC = 0.070Z^{0.74}$, where IWC is in g m^{-3} and Z in

* *Corresponding author address:* Eun-Kyoung Seo, Florida State Univ., Dept. of Meteorology, Tallahassee, FL 32306-4520; email: ekseo@met.fsu.edu.

$mm^6 m^{-3}$ and then summed in the vertical to obtain columnar ice water content (that is, ice water path). Overall the NEXRAD retrievals exhibit larger IWPs than the AMSU-B retrievals. It can be partly attributed to large volume sampling by NEXRAD in distant range from the KINX radar site and coarse resolution in the vertical. In a large volume some large-sized ice particles can contribute large reflectivity factor to the whole volume because of the sixth power of diameters of the water equivalent drops for ice particles per unit volume of air (Battan 1973). The AMSU-B retrievals have relatively lower IWPs due to large footprints, where there is presumably underestimation of IWPs due to nonlinearity of T_B-IWP relations and inhomogeneity. In spite of some discrepancies in IWP amounts between the two measurements, the horizontal structures of the events from the measurements are in a good agreement and the AMSU-B retrievals capture main features of the cloud systems viewed by the KINX NEXRAD.

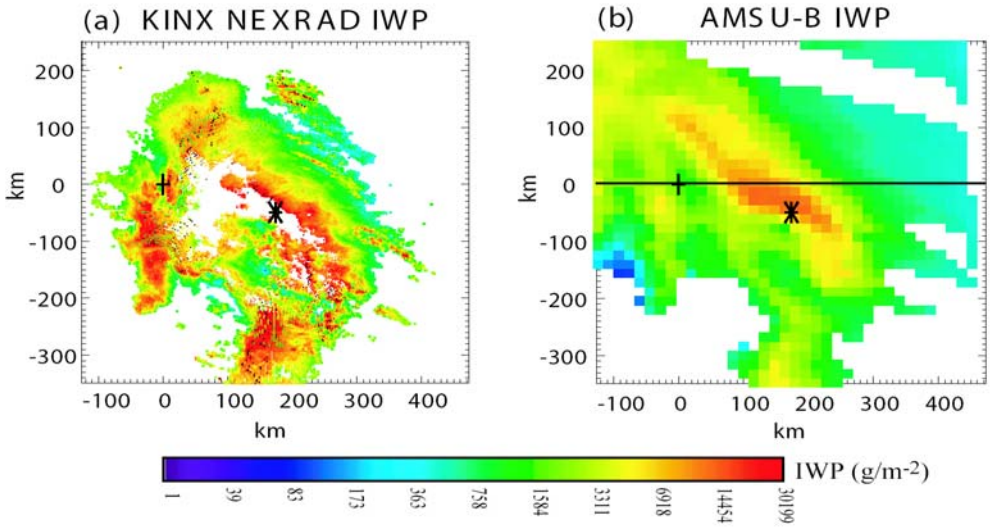

Figure 1. Horizontal IWP distribution from (a) the NEXRAD and (b) the AMSU-B retrievals on 2 March 2000. Cross and asterisk in each panel represent the SGP site and KINX site, respectively. In the NEXRAD IWP, white pixels within echoes denote radar reflectivity greater than 30 dBZ within their cloud column.

5. VERTICAL STRUCTURE OF AMSU-B AND MMCR IWCS

Figure 2 shows the vertical structures of the AMSU-B and MMCR IWC retrievals for three cases, representing moderate, moderately weak, and weak cases. On 2 March 2000, the spatial scale along the cross section is about 450 km and the time scale is about 6.5 hours (Figs. 2ad). The spatial scale is likely congruous with the time scale for the system movement with ~15 m s^{-1}. Overall vertical structures retrieved from the two measurements are quite similar to each other with respect to anvil in front of the cloud system, convective clouds and trailing stratiform clouds, and cloud top height. The amounts of IWC from the AMSU-B observations are larger than those from the MMCR observations in cloud columns between 50 km and 200 km. This can be partly attributed to that some cells in the cloud system developed in time into stronger radar reflectivity after passing through the SGP site.

The second case on 22 March 2000 is moderately weak, having radar echoes confined in low-to-middle layers in the MMCR observations. The time scale (about 1.5 hours) is relatively short compared to the event on 2 March 2000 (Figs. 2bd). The retrieved ice clouds exhibit quite analogous cloud structures, having maximum ice water contents at lower-to-mid layer between 15-80 km in space cross-section of the AMSU-B retrievals and day number 82.57-82.54 in time cross-section of the MMCR retrievals. Middle layer maximum is well matched between 80-140 km in space cross-section and day number 82.54-82.51

in time cross-section. On the other had, the AMSU-B tends to retrieve more broadly distributed ice water contents (near 0.001 g m^{-3}) in the vertical.

The third case has weak radar reflectivity confined in relatively lower layers. In general, the AMSU-B retrieves IWCs in broader range in the vertical compared to the MMCR observations (Figs. 2cf). Given comparison between space and time, the retrievals from the AMSU-B observations seem to be quite compatible with those from the MMCR.

For the month of March, there are about 60 collocated cases of the AMSU-B and MMCR observations. The AMSU-B and MMCR retrievals were area-averaged over 0.25° serach range centered at the SGP site and time-averaged over 90-minutes centered at the AMSU-B collocation time. With the collocated profiles whose IWPs are greater than 10 g m^{-3}, mean IWC profiles are plotted in Fig. 3. Overall, the mean AMSU-B profile captures well the vertical trends of the mean MMCR profile even though different circumstances exist between the two different measurements such as: (1) 3-dimensional clouds from AMSU-B vs. 2-dimensional clouds from MMCR, (2) spatial average from AMSU-B vs. temporal average from MMCR, and (3) scenes from slantwised viewing angles in AMSU-B vs. scenes from nadir in MMCR.

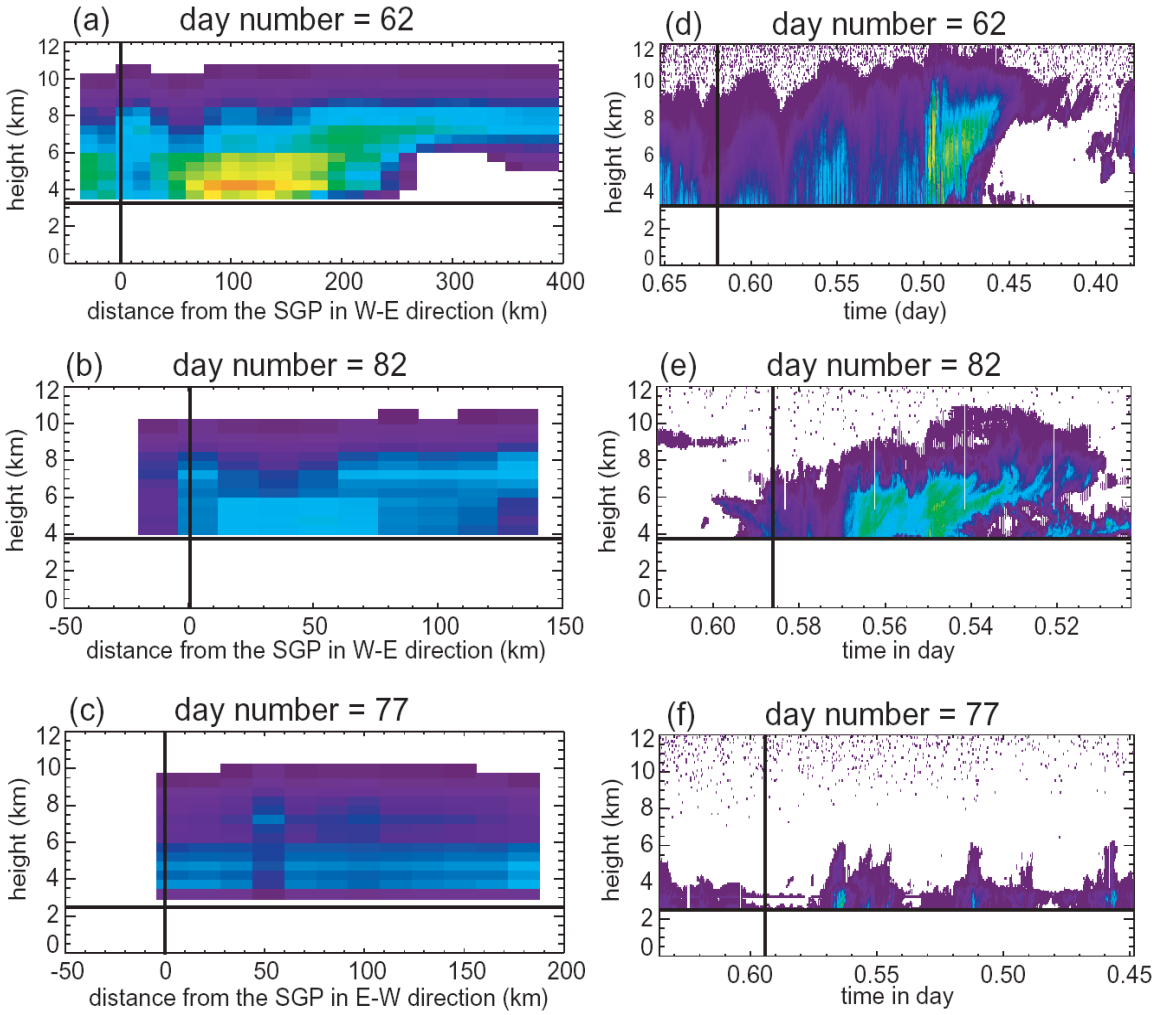

Figure 2. Vertical IWC structures retrieved from (a-c) AMSU-B TBs along the West-East cross section located in Figure 1 and (d-f) MMCR along the time cross section on each day number. The vertical solid lines in (a-c) and (d-f) represent, respectively, the SGP site in space and the AMSU-B satellite observation time at the SGP site.

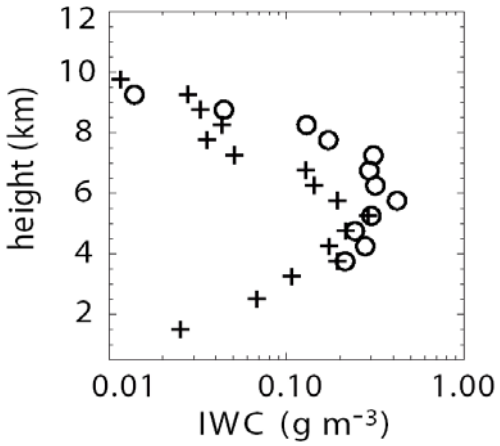

Figure 3. Mean MMCR- (crosses) and AMSU-B-based (circles) IWC profiles. The MMCR time window and AMSU-B search range are 90-minutes and 0.25º, respectively.

6. DISCUSSIONS

The IWC profiles retrieved from AMSU-B are in a good agreement with the MMCR and the NEXRAD observations with respect to both horizontal and vertical structures of ice cloud water content. The results are encouraging in fulfillment of the need of SCMs (that is, advection tendency of cloud condensates). On the other hand, it seems to be very challenging to retrieve ice clouds with small amounts of IWC only from AMSU-B observations.

ACKNOWLEDGEMENTS

Data were obtained from DOE ARM Program.

REFERENCES

Battan, L. J., 1973: Radar Observation of the Atmosphere. Chicago, University of Chicago Press, 324 pp.

Liu, G., 2004: Approximation of single scattering properties of ice and snow particles for high microwave frequencies, *J. Atmos. Sci.*, **61**, 2441-2456.

Olson, W. S., C. D. Kummerow, G. M. Heymsfield, and L. Giglio, 1996: A method for combined passive-active microwave retrievals of cloud and precipitation profiles. *J. Appl. Meteor.*, **35**, 1763-1789.

Randall, D. A., K.-M. Xu, R. J. C. Somerville, and S. Iacobellis, 1996; Single-column models and cloud ensemble models as links between observations and climate models, *J. Clim*., **9**, 1683-1697.

Seo, E.-K. and Guosheng Liu, 2005; Retrievals of Cloud Ice Water Path by Combining round Cloud Radar and Satellite High-Frequency Microwave Measurements Near The ARM SGP Site, *J. Geophys. Res.*, *110*, D14203, doi:10.1029/ 2004JD005727.